Hindawi
Complexity
Volume 2020, Article ID 9861642, 10 pages
https://doi.org/10.1155/2020/9861642

Research Article

Adaptive Chebyshev Neural Network Control for Ventilator Model under the Complex Mine Environment

Ranhui Liu, Xinyan Hu, Chengyuan Zhang, and Chuanxi Liu

Intelligent Equipment Academy, Shandong University of Science and Technology, Tai'an 271019, China

Correspondence should be addressed to Ranhui Liu; liuranhui@sdust.edu.cn

Received 5 July 2020; Accepted 21 July 2020; Published 27 August 2020

Guest Editor: Shubo Wang

Ventilator is important equipment for mines as it safeguards the lives under the shaft and ensures other equipment's proper functioning by providing fresh air. Therefore, how to effectively control the ventilator system becomes more significant. In order to acquire the commonly used model and control strategy for ventilator systems, a new universal ventilator model is established based on the blast capacity differential pressure in the ventilating duct and the ventilator motor model. Then, an adaptive Chebyshev neural network (ACNN) controller is proposed to effectively control the ventilator system where the unknown load torque and the unknown disturbance caused by the complex environment under the shaft are approximated by the Chebyshev neural network (CNN). Afterwards, an appropriate Lyapunov function candidate is designed to guarantee the stability of the proposed controller and the closed-loop ventilator system. Finally, the ACNN controller has been demonstrated to be effective in terms of validity and precision for the new proposed ventilator model through the simulations.

1. Introduction

The ventilator motor is very important for the mine since it is the core equipment supporting the fresh air under the shaft [1–7]. Controlling the ventilator motor is always the most important issue in the process of mining. In order to precisely control the ventilator for saving the energy, the ventilator model must be investigated firstly. It has several kinds of models (ARMA model, computational fluid dynamics model, etc.) for ventilator systems so far, but all are suiting special conditions in special systems. Then, investigating the universal ventilator system model for mines is of significance. Zhang et al. [2] investigated a train tunnel model based on big data. The ventilation system was adjusted and regulated by iterative learning control algorithm and the results demonstrated the proposed control method was superior to active control. Roubłk et al. [6] investigated a mechanical ventilation for lung injury aimed at preservation of spontaneous breathing when using high-frequency oscillatory (HFO) ventilators, who designed a linear quadratic Gaussian state feedback controller to compensate for the changes in mean airway pressure (MAP) in the ventilator circuit caused by spontaneous breathing. Different from Zhang et al. [2] and Roubłk et al. [6], Yan et al. [7] investigated the high-altitude ventilator motor model for stratospheric airship airbags. They extended the traditional minimum stator current operation to minimize conduction below the rated speed concept, where an extended minimum stator current operation (EMSCO) was designed at any speed to formalize as constrained optimization problem. Then, they proposed optimal duty cycle model predictive current control (ODC-MPCC) to reduce the current ripple and computation burden. From these references, one can find that most control strategies were based on optimal control. But the mine environment even under the shaft is so intricate that many elements can disturb the optimal control strategy. Therefore, the optimal controller will not acquire the desired results under the complex disturbance in the mine. It needs a new control strategy for the ventilator motor suiting the complex environment of the mine, especially under the shaft.

Adaptive control is an intelligent control strategy which can solve most nonlinear complex issues [8–18]. In this paper, we will adopt adaptive control for the ventilator motor to restrain the strong nonlinear influence caused by

the complicated, noisy, and dusty environment of the mine. There are a lot of researchers applying the adaptive control to solve the nonlinear issues. Chen et al. [19] proposed a fixed-time adaptive control for buck DC/DC converters. An adaptive update law was adopted to estimate all the unknown parameters of the buck converters, and the fixed-time sliding mode surface (SMS) and corresponding control were developed for the buck converters with known parameters such that the output error would converge to the equilibrium point within a fixed time. Gao et al. [14] investigated the discrete Hammerstein system with Preisach hysteresis nonlinearity and unknown order linear dynamics. They proposed a lower triangular matrix to identify the Preisach density function and adopted Hankel matrix estimating the linear dynamics order. Then, a composite control consisting of discrete inverse model-based controller (DIMBC) and discrete adaptive sliding mode controller (DASMC) was proposed to deal with the Hammerstein system which can reduce the reaching time of DASMC and improve the robustness of DIMBC. Sun et al. [16] designed a feedback adaptive controller for controlling the backlash servo system. Firstly, an extended state observer (ESO) was adopted to estimate the system states and the vibration torque. Then, considering the feedback and feedforward signals, an adaptive robust compensation controller was designed for this backlash servo system and the experiment results have demonstrated the effectiveness for the systems. Different from former researchers, Wang et al. [17] applied the adaptive method to estimate the unknown parameters rather than using it as controller. Then, considering the problem for the sluggish convergence caused by the online learning, this study proposed a new adaptive law to achieve optimal parameter estimation. In order to achieve this purpose, an auxiliary filter was designed to compel the adaptive law with a time-varying gain under a cost function. Finally, an adaptive nonsingular terminal sliding mode control (ANTSMC) was proposed for a considered servo system to obtain tracking control and parameter estimation simultaneously. Na et al. [20] considered an energy maximization problem for wave energy converters (WECs) subject to nonlinearities and constraints. The adaptive approach was used to solve the Hamilton–Jacobi–Bellman equation and a critic neural network (NN) to approximate the time-dependent optimal cost value. They combined the adaptive control and optimal control to deal with the wave energy converters (WECs). From these studies, it shows that the adaptive control can perfectly be adopted for the nonlinear systems with adaptive update law; even so, some unknown nonlinear sections or disturbances or models will also be estimated by other methods, such as fuzzy logic [21] and neural network [22–25].

The Chebyshev neural network (CNN) is a functional-link neural network that is a single-layer neural structure with less computation to estimate the nonlinear function [26–30]. It has been utilized to estimate most kinds of uncertain linear or nonlinear sections. Zou et al. [26] used the Chebyshev neural network for approximating the spacecraft attitude motion in uncertain spacecraft systems. They proposed Chebyshev neural network controller-I and adaptive NN controller-II for global representation without singularities of the systems. Different from Zou et al. [26], Gao and Liu [27] investigated a backlash-like hysteresis nonlinear system using the multiscale Chebyshev neural network (MSCNN) method to identify the unknown hysteresis nonlinearity. Firstly, the unknown hysteresis backlash-like nonlinearity would be approximated by the new multiscale Chebyshev neural network. Then, the tracking error was transformed into scalar error by Laplace transformation to simplify the computation. Finally, an adaptive control was designed for controlling the backlash-like hysteresis nonlinear system, and the simulations verified the effectiveness of the multiscale Chebyshev neural network identification and the adaptive controller. Sun et al. [28] focused on the multimotor servomechanism with unmodeled dynamics. An extended state observer based on high-order sliding mode (HOSM) differentiator was applied for unmeasured velocity, and the Chebyshev neural network was adopted to deal with the friction and disturbances. The experiments proved that the proposed approach was useful. To sum up, the Chebyshev neural network was utilized for different nonlinear systems and obtained good results. Therefore, we will utilize the CNN to deal with the unknown nonlinear complex uncertain sections in the ventilator system in this paper.

Firstly, a new ventilator model will be established based on the blast capacity differential pressure of the ventilating duct and the ventilator motor, that is, a nonlinear dynamic model where some load torques and some complex disturbances are unknown. Then, a Chebyshev neural network will be designed to estimate the unknown nonlinear section and an adaptive CNN controller will be proposed for the closed-loop ventilator system. Finally, the appropriate Lyapunov function guarantees the convergence of the closed-loop ventilator system and the simulations also affirm that the proposed approach is precise and effective.

This paper is organized as follows. Section 2 gives the problem formulations, which introduces the proposed ventilator model based on the blast capacity differential pressure and the ventilator motor and also introduces the structure of the Chebyshev neural network. Section 3 presents the controller design, that is, the process to the design control. The stability of the ventilator system by Lyapunov function is also given in this section. Then, simulations are given in Section 4, and Section 5 concludes the paper.

2. Problem Formulations

2.1. The Ventilator Model. The most important index of the ventilator model is the flux of the ventilating duct. Considering the complicated and dusty environment of the ventilating duct in the mine, the approach of the blast capacity differential pressure is selected to solve the fresh air velocity measurement hole blocking in order to realize the real-time accuracy measurement and monitor the wind pressure. The schematic diagram structure of the blast capacity differential pressure method is illustrated in Figure 1. From Figure 1, the energy equations of sections I and II can be deduced as follows:

$$\begin{cases} p_{s1} + \rho_1 Z_1 g + \dfrac{\rho_1 v_1^2}{2} = p_{s2} + \rho_2 Z_2 g + \dfrac{\rho_2 v_2^2}{2} + h_r, \\ p_{s1} + \rho_1 Z_1 g + \dfrac{\rho_1 v_1^2}{2} = p_{s2} + \rho_2 Z_2 g + \dfrac{\rho_2 v_2^2}{2} + \xi \dfrac{\rho v_2^2}{2}, \end{cases} \tag{1}$$

where $p_{s1}, p_{s2}, \rho_1, \rho_2, Z_1, Z_2, v_1, v_2$ represent the static pressure, air density, elevation, and air speed of sections I and II, respectively, h_r is the local resistance of section II, and ξ is the coefficient of local resistance of section II.

Since sections I and II have close distance and same elevation, $\rho = \rho_1 = \rho_2 = Z_1 = Z_2$ holds. Considering the equation (1), we have

$$p_{s1} - p_{s2} = \frac{\rho v_2^2}{2} - \frac{\rho v_1^2}{2}. \tag{2}$$

Since sections I and II have close distance, the air volume of ventilating duct Q can be deduced as

$$Q = Q_1 = Q_2, \tag{3}$$

where Q_1, Q_2 represent the air volume of sections I and II, respectively.

Substituting $v_1 = Q/s_1, v_2 = Q/s_2$ into equation (2), we obtain

$$\begin{aligned} Q &= s_1 s_2 \sqrt{\frac{2(p_{s1} - p_{s2})}{\rho(s_1^2 - s_2^2)}}, \\ s_1 &= \frac{\pi d_1^2}{4}, \\ s_2 &= \frac{\pi(d_2^2 - d_1^2)}{4}, \end{aligned} \tag{4}$$

where s_1, s_2 represent the areas with the different definition in (4), respectively, and d_1, d_2 mean outer diameter and insider diameter of the fairing, respectively. From equation (4), the ventilator air volume flow can be calculated where $\rho, s_1, s_2, p_{s1}, p_{s2}$ is measured by the different sensors. Based on reference [7], it is obvious that the effective control for ventilator motor will save energy and control the air volume flow Q. Therefore, an effective control strategy for ventilator motor will effectively control the ventilator air volume flow. The ventilator motor model in D-Q coordinates is represented as follows:

$$\begin{bmatrix} \dot{d} \\ \ddot{q} \end{bmatrix} = \begin{bmatrix} -\dfrac{R}{L} & \dfrac{K}{L} \\ \dfrac{K_t}{J_i} & \dfrac{1}{J_i} \end{bmatrix} \begin{bmatrix} i_q \\ \dot{q} \end{bmatrix} + \begin{bmatrix} \dfrac{u_q}{L} \\ -\dfrac{T_n + T_l}{L} \end{bmatrix}, \tag{5}$$

where R, L represent the stator resistance and inductance, respectively. $K = n\psi$, n is the number of the pole pairs, ψ is the rotor flux linkage, K_t, J_i, u_q are the torque constant, inertia, and q-axis stator voltages, respectively. T_n is the torque caused by some nonlinear portion such as friction, disturbance, and so on. $T_l = f(Q)$ is the load torque which is the unknown function about ventilator air volume flow in this paper.

Define $x = [x_1, x_2]^T = [q, \dot{q}]^T$; based on reference [31], ventilator motor model (5) can be rewritten as

$$\begin{aligned} \begin{bmatrix} \dot{x}_1 \\ \dot{x}_2 \end{bmatrix} &= \begin{bmatrix} 0 & 1 \\ 0 & \dfrac{KK_t}{J_i R} \end{bmatrix} \begin{bmatrix} x_1 \\ x_2 \end{bmatrix} + \begin{bmatrix} 0 \\ \dfrac{K_t u_q - T_n R - R f(Q)}{J_i R} \end{bmatrix}, \\ y &= x_1. \end{aligned} \tag{6}$$

2.2. Chebyshev Neural Network. In this section, a CNN will be designed to estimate the unknown sections in equation (6). CNN is one of the functional-link neural networks whose structure is illustrated in Figure 2. From Figure 2, CNN is a single-layer neural network which relies on the Chebyshev polynomials. Therefore, it has lower computation and is widely used for function estimation.

The CNN can be defined as follows:

$$F(x) = W^* \Psi(x) + \zeta, \tag{7}$$

where W^* is the weight matrix of the CNN and ζ is the bounded approximation error for the CNN.

$$\begin{aligned} \Psi(x) = [1, d_1(x_1), d_2(x_1), \ldots, d_m(x_1), d_1(x_2), d_2 \\ \cdot (x_2), \ldots, d_m(x_2), \ldots, d_1(x_n), d_2(x_n), \ldots, d_m(x_n)]^T, \end{aligned} \tag{8}$$

where $[x_1, x_2, \ldots, x_n]^T$ is the n-dimensional input vector, m represents the order of the Chebyshev polynomial, and the Chebyshev polynomial $d_k(x_l)$ is defined as the two-term recursive formula as follows:

$$d_k(x_l) = 2x_l d_{k-1}(x_l) - d_{k-2}(x_l), \tag{9}$$

where the original value of $d(x)$ is selected as $d_1(x_l) = x_l, d_0(x_l) = 1$.

The CNN update law is defined as follows:

$$\dot{\widehat{W}} = -\frac{\varrho_3}{2} e_2 \Psi(x), \tag{10}$$

where ϱ_3 is the designed positive constant, e_2 is defined in (16), and $\widehat{W}$ is the estimation of the weight W^*.

3. Controller Design

Considering the structure of the ventilator models (1) and (6), we should design a recursive control strategy to solve the problem. The recursive controller method is designed as follows.

Step 1: in order to design the U-model CNN adaptive controller, the output error is defined as follows:

$$e = y - y_d, \tag{11}$$

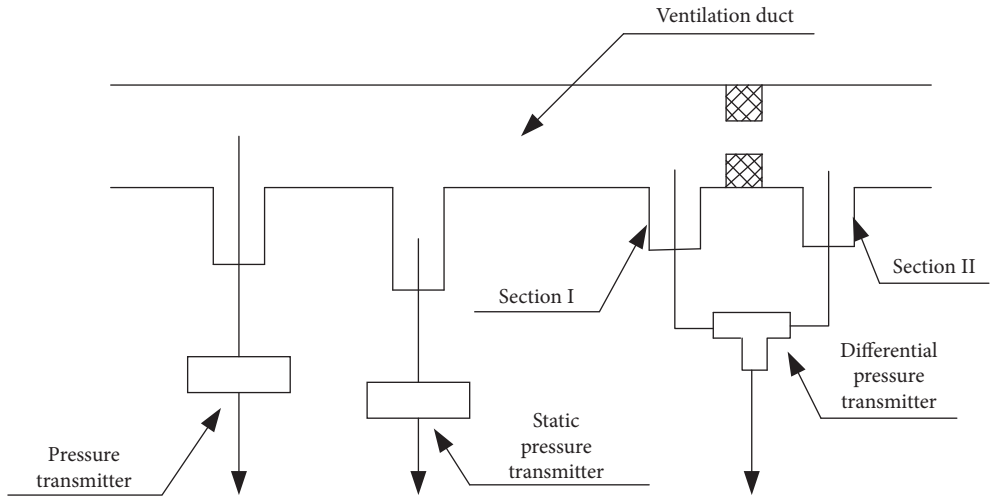

Figure 1: The structure of the blast capacity differential pressure.

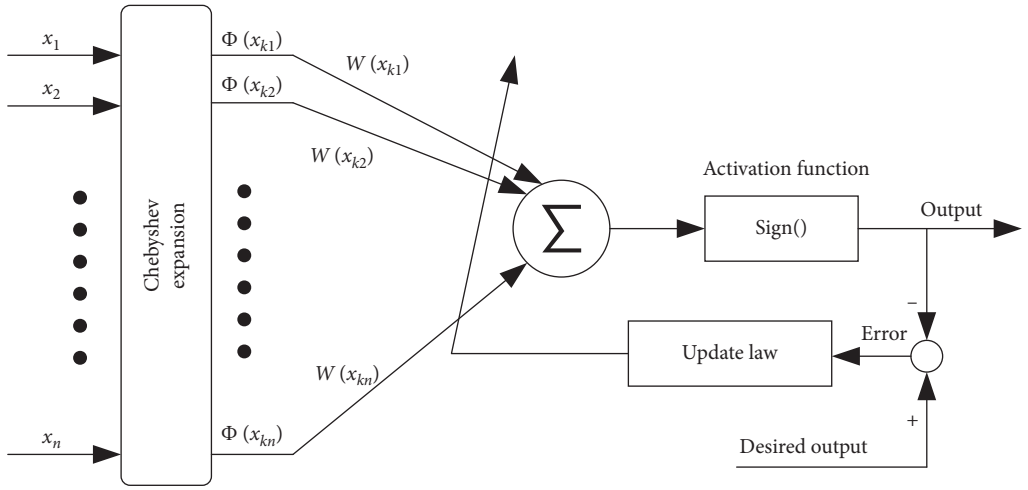

Figure 2: The structure of the Chebyshev neural network.

where y_d is a known signal which has $(m+1)$th derivative such as a sinusoidal signal.

Considering equation (6), the derivative of e can be deduced as

$$\begin{aligned} \dot{e} &= \dot{y} - \dot{y}_d \\ &= \dot{x}_1 - \dot{y}_d \\ &= x_2 - \dot{y}_d. \end{aligned} \tag{12}$$

Assume T_n and $f(Q)$ are unknown, where T_nR and $Rf(Q)$ are estimated by the CNN. Then, the 2th derivative of e is obtained as

$$\begin{aligned} \ddot{e} &= \dot{x}_2 - \ddot{y}_d \\ &= \frac{KK_t}{J_iR}x_2 + \frac{K_tu_q - T_nR - Rf(Q)}{J_iR} - \ddot{y}_d \\ &= \frac{KK_t}{J_iR}x_2 + \frac{K_t}{J_iR}u_q - W^*\Psi(x) - \ddot{y}_d. \end{aligned} \tag{13}$$

Define the following Lyapunov function candidate as

$$V_1 = \frac{1}{2}e^2. \tag{14}$$

Then, the derivate of V_1 can be deduced as

$$\dot{V}_1 = e\dot{e} = e(x_2 - \dot{y}_d). \tag{15}$$

In this step, x_2 is treated as a virtual input; therefore, we define an error as $e_2 = x_2 - a_2$, where a_2 is a virtual control law. Substitute $x_2 = e_2 - a_2$ into (15), and we have

$$\dot{V}_1 = e(e_2 - a_2 - \dot{y}_d). \tag{16}$$

Define the virtual control law a_2 as follows:

$$a_2 = l_1e - \dot{y}_d + e_2, \tag{17}$$

where l_1 is a positive feedback control gain, and we can go to the next step.

Step 2: the actual controller u will be acquired in this step. Firstly, we define the derivative of e_2 as

$$\dot{e}_2 = \dot{x}_2 - \dot{a}_2. \tag{18}$$

Based on (17), the derivation of a_2 is deduced as

$$\begin{aligned} \dot{a}_2 &= l_1\dot{e} - \ddot{y}_d + \dot{e}_2 \\ &= l_1\left(e_2 - a_2 - \dot{y}_d\right) - \ddot{y}_d + \dot{e}_2, \end{aligned} \tag{19}$$

and then substituting (19) into (18), one can get

$$\dot{e}_2 = \frac{1}{2}\left(\frac{KK_t}{J_iR}x_2 + \frac{K_t}{J_iR}u_q - W^*\Psi(x) - l_1e_2 + l_1a_2 + l_1\dot{y}_d + \ddot{y}_d\right). \tag{20}$$

Define the adaptive update errors as

$$\begin{aligned} \tilde{a}_2 &= a_2 - \hat{a}_2, \\ \tilde{x}_2 &= x_2 - \hat{x}_2, \\ \tilde{W} &= W^* - \hat{W}, \end{aligned} \tag{21}$$

where $\hat{a}_2, \hat{x}_2$ are the estimations of a_2, x_2.
The adaptive update law is defined as follows:

$$\begin{aligned} \dot{\hat{x}}_2 &= \frac{\varrho_1}{2}\frac{KK_t}{J_iR}e_2, \\ \dot{\hat{a}}_2 &= \frac{\varrho_2}{2}l_1e_2, \end{aligned} \tag{22}$$

where ϱ_1, ϱ_2 are designed positive constants.
We select the true controller input as

$$u_q = \frac{J_iR}{K_t}\left(-\frac{KK_t}{J_iR}\hat{x}_2 + \hat{W}\Psi(x) - l_1\hat{a}_2 - l_1\dot{y}_d - \ddot{y}_d\right). \tag{23}$$

Select the Lyapunov function candidate as follows:

$$V = \frac{1}{2}e_2^2 + \frac{1}{2\varrho_1}\tilde{x}_2^2 + \frac{1}{2\varrho_2}\tilde{a}_2^2 + \frac{1}{2\varrho_3}\tilde{W}^T\tilde{W}. \tag{24}$$

The derivative of V is deduced as

$$\dot{V} = e_2\dot{e}_2 + \frac{1}{\varrho_1}\tilde{x}_2\dot{\tilde{x}}_2 + \frac{1}{\varrho_2}\tilde{a}_2\dot{\tilde{a}}_2 + \frac{1}{2\varrho_3}\tilde{W}^T\dot{\tilde{W}}. \tag{25}$$

Substituting (20) into (25), the derivative of V can be deduced as

$$\begin{aligned} \dot{V} = \frac{e_2}{2}&\left(\frac{KK_t}{J_iR}x_2 + \frac{K_t}{J_iR}u_q - W^*\Psi(x) - l_1e_2 + l_1a_2 + l_1\dot{y}_d + \ddot{y}_d\right) \\ &+ \frac{1}{\varrho_1}\tilde{x}_2\dot{\tilde{x}}_2 + \frac{1}{\varrho_2}\tilde{a}_2\dot{\tilde{a}}_2 + \frac{1}{2\varrho_3}\tilde{W}^T\dot{\tilde{W}}. \end{aligned} \tag{26}$$

Substituting the true controller (23) into (26), one can obtain

$$\begin{aligned} \dot{V} = \frac{e_2}{2}&\left(\frac{KK_t}{J_iR}x_2 - \frac{KK_t}{J_iR}\hat{x}_2 - W^*\Psi(x) - l_1e_2 + l_1a_2 + l_1\dot{y}_d \right. \\ &\left. + \ddot{y}_d + \hat{W}\Psi(x) - l_1\hat{a}_2 - l_1\dot{y}_d - \ddot{y}_d\right) + \frac{1}{\varrho_1}\tilde{x}_2\dot{\tilde{x}}_2 \\ &+ \frac{1}{\varrho_2}\tilde{a}_2\dot{\tilde{a}}_2 + \frac{1}{2\varrho_3}\tilde{W}^T\dot{\tilde{W}} \\ = -\frac{1}{2}&l_1e_2^2 + \frac{e_2}{2}\left(\frac{KK_t}{J_iR}\tilde{x}_2 + \tilde{W}\Psi(x) + l_1\tilde{a}_2\right) - \frac{1}{\varrho_1}\tilde{x}_2\dot{\hat{x}}_2\frac{1}{\varrho_2}\tilde{a}_2\dot{\hat{a}}_2 \\ &- \frac{1}{\varrho_3}\tilde{W}^T\dot{\hat{W}}. \end{aligned} \tag{27}$$

Substituting (10) and (22) into (27), according to Lyapunov theory, one can obtain that the closed loop is stable with the designed CNN adaptive controller.

4. Simulation

The simulations is designed to verify the effectiveness of the ventilator motor in the mine. In the simulations, the ventilator model parameters are listed in Table 1. The parameters of the ventilator motor model in D-Q coordinates are listed in Table 2. The reference input is selected as $y_d = \sin(t)$. The simulation results are shown in Figures 3–12. From Figures 3–7, it is clearly shown that the proposed control strategy is effective.

Figure 3 shows the control results with the proposed neural network adaptive controller. The controlled output can quickly track the reference input with smaller and convergent error which is also shown in Figure 4. From Figure 4, it is very obviously illustrated that the error is converged and the mean absolute error (MAE) is less than 0.02. Figure 5 shows the controller input, and it shows the same conclusions compared with Figures 3 and 4. From Figure 5, the dynamic process can be clearly shown less than 1 second in these simulations, and then the neural network and the adaptive update law can estimate the unknown nonlinear section and parameters quickly. The tracking result is clearly shown in Figure 3. Figures 6 and 7 show the trajectories for the estimation $\hat{x}_1, \hat{x}_2$ of x_1 and x_2. From these two diagrams, it can be concluded that the proposed method can estimate the system state rapidly and the tracking controller is effective, which are in line with the results in Figures 3–5.

To magnify the amplitude of the input signal, the results are shown in Figures 8–12. From Figures 8 and 9, one can have the same conclusions compared with Figures 3 and 4. But comparing Figure 10 with Figure 5, it is clearly illustrated that Figure 10 has more drastic change. Then, comparing Figures 3–5 with Figures 8–10, it is illustrated that magnifying the signal amplitude will influence the controlled input, but the proposed controller also retains the control precision with strong control input. Figures 11 and 12 also show the same conclusion.

Table 1: The parameters of the ventilator.

Parameters	Value	Units
p_{s1}	1.51	kPa
p_{s2}	1.52	kPa
ρ_1	1	kg/m^3
ρ_2	1	kg/m^3
Z_1	−50	m
Z_2	−50	m
v_1	10	m/s
v_2	10	m/s
h_r	150	N
s_1	0.2	m^2
s_2	0.001	m^2
ξ	0.8	

Table 2: The parameters of the ventilator motor in D-Q coordinates.

Parameters	Value	Units
J_s	0.01	
K	0.5	
K_t	10	
R	0.1	kΩ
T_n	0.02	Nm

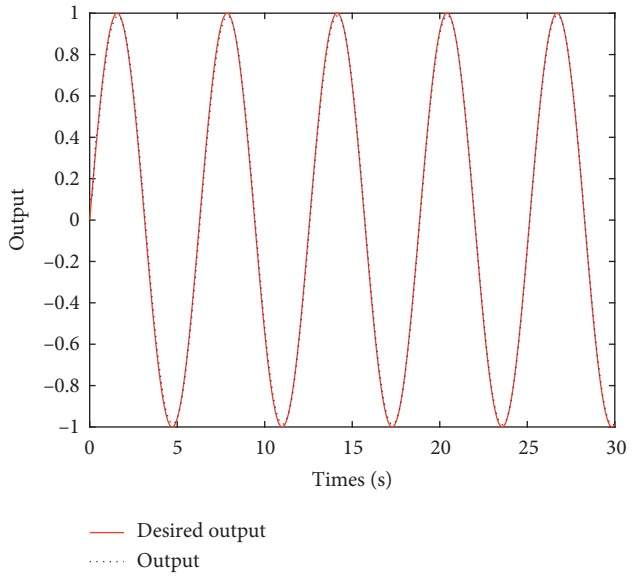

Figure 3: The control results with small input signal amplitude.

Remark 1. In this paper, since the controller is designed based on the output tracking error, the tracking control results are excellent in Figures 3 and 8. But in Figures 7 and 12, the system states x_1, x_2 have a chattering. The reason is that we did not consider the state control and we also did not utilize the state observer. Then, the tracking error can affect the system states by the feedback structure that makes some chattering in the system states. We will further investigate this phenomenon in the future work.

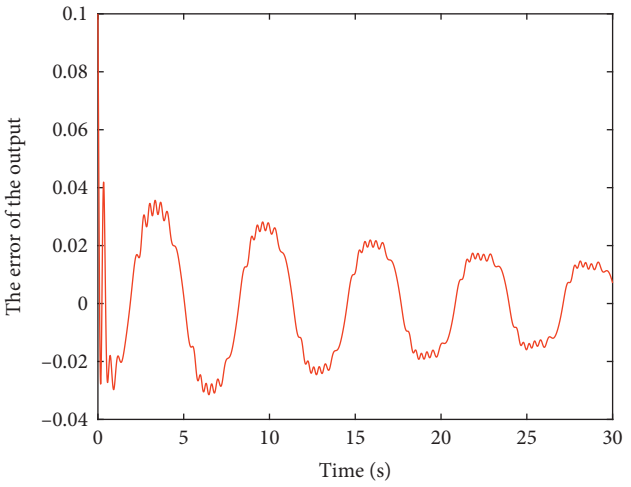

Figure 4: The errors of output with small input signal amplitude.

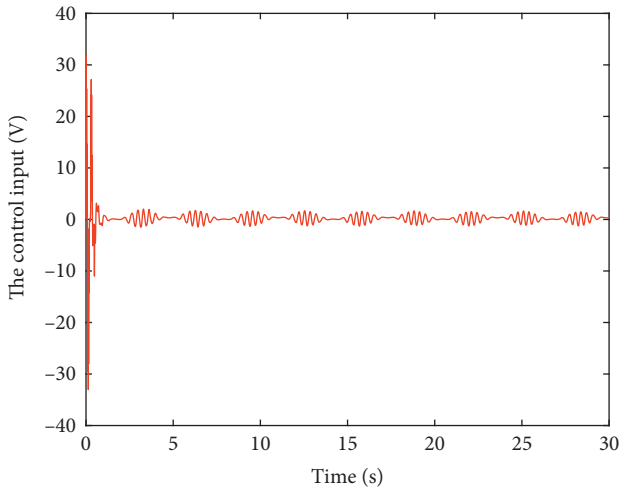

Figure 5: The trajectory of the controller input.

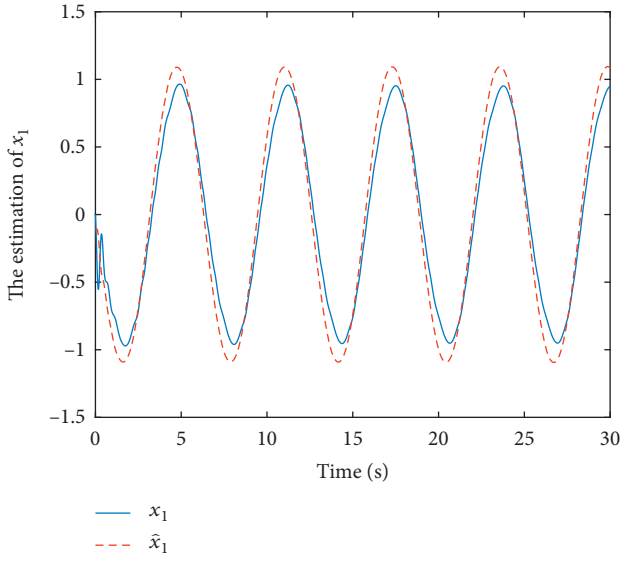

Figure 6: The estimation of x_1.

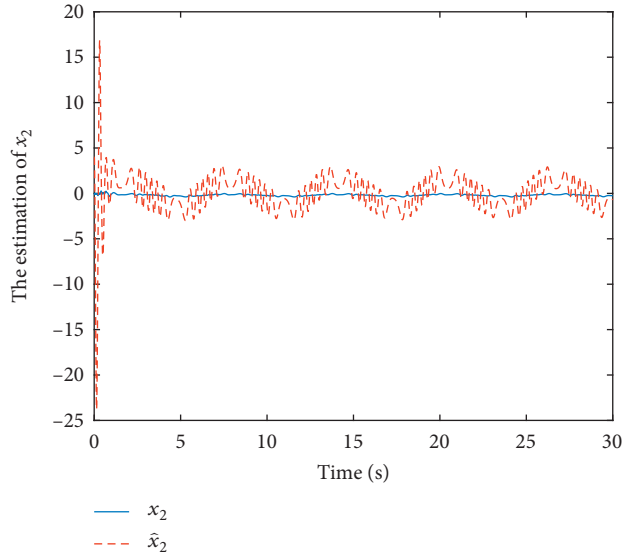

Figure 7: The estimation of x_2.

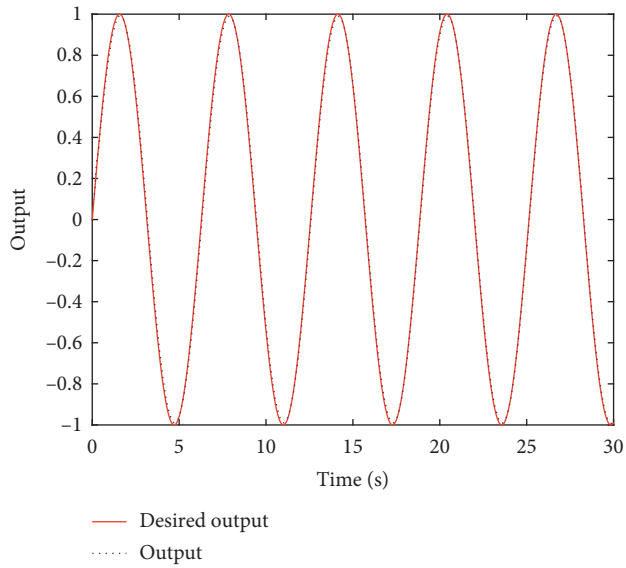

Figure 8: The control results with large input signal amplitude.

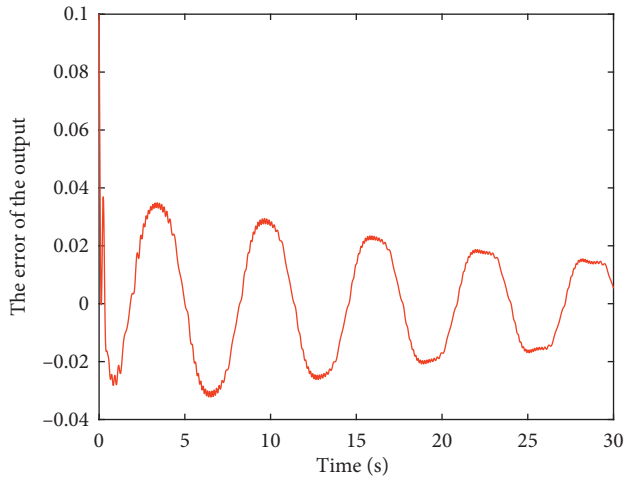

Figure 9: The errors of output with large input signal amplitude.

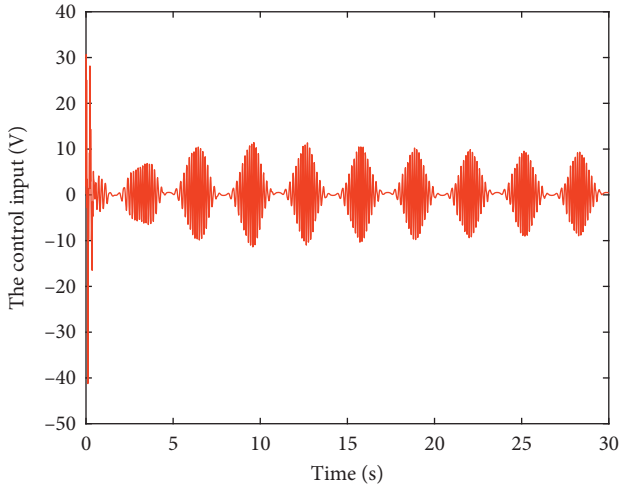

Figure 10: The trajectory of the controller input.

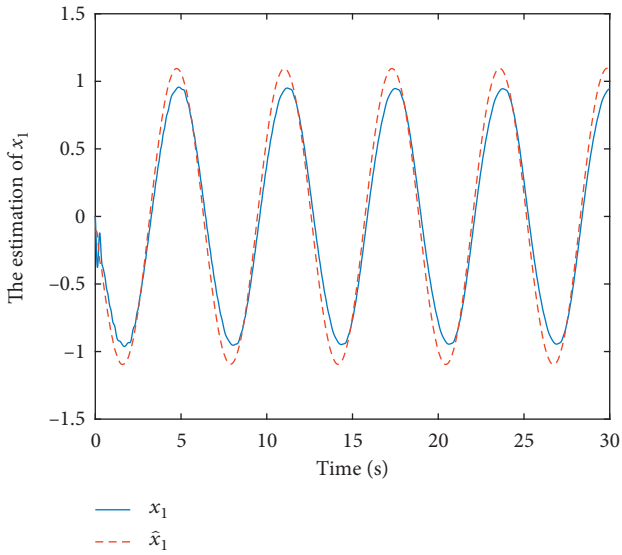

Figure 11: The estimation of x_1.

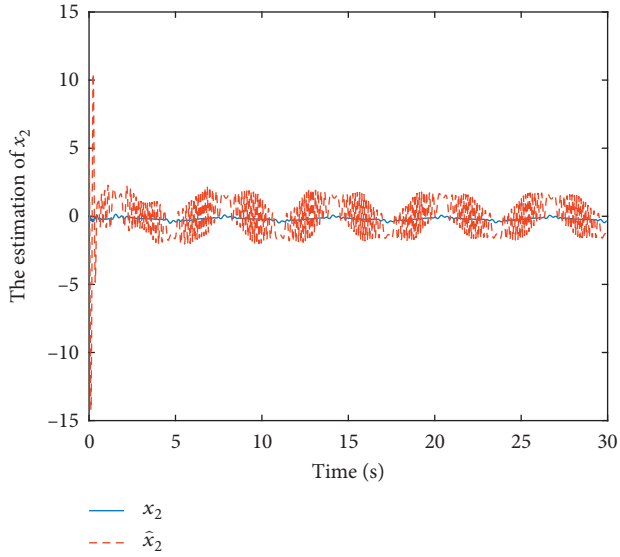

Figure 12: The estimation of x_2.

5. Conclusion

A new adaptive Chebyshev neural network (ACNN) control was presented to precisely control the ventilator system in this paper. Considering that the optimal controller does not suit the complex environment under the shaft in the mine which is easily affected by the strong disturbance caused by the hostile environment, the ACNN replaced the optimal control compared with other traditional control strategies. Firstly, the new ventilator model was proposed which consisted of the blast capacity differential pressure equation in the ventilator duct and the ventilator motor equation. Then, the CNN estimated the unknown nonlinear sections such as the unknown load torque and the unknown disturbance caused by the hostile environment under the shaft. Finally, the stability of the closed-loop ventilator system was guaranteed by a designed appropriate Lyapunov function candidate and the simulation results verified the effectiveness and the precision of the established new ventilator model and the presented ACNN control strategy.

Data Availability

No data were used to support this study.

Conflicts of Interest

The authors declare that they have no conflicts of interest.

Acknowledgments

This study was supported by the Shandong Provincial Key Research and Development Project (2019GGX101005), Shandong Provincial Natural Science Foundation (ZR2017MF048), and National Natural Science Foundation of China (61803216).

References

[1] A. Das, P. P. Menon, J. G. Hardman, and D. G. Bates, "Optimization of mechanical ventilator settings for pulmonary disease states," *IEEE Transactions on Biomedical Engineering*, vol. 60, no. 6, pp. 1599–1607, 2013.

[2] Y. Zhang, J. Su, and M. Chen, "Research on adaptive iterative learning control of air pressure in railway tunnel with IOTs data," *IEEE Access*, vol. 8, pp. 5481–5487, 2020.

[3] P. Casaseca-de-la-Higuera, F. Simmross-Wattenberg, M. MartIn-Fernandez, and C. Alberola-Lopez, "A multichannel model-based methodology for extubation readiness decision of patients on weaning trials," *IEEE Transactions on Biomedical Engineering*, vol. 56, no. 7, pp. 1849–1863, 2009.

[4] H.-T. Wu, S.-S. Hseu, M.-Y. Bien, Y. R. Kou, and I. Daubechies, "Evaluating physiological dynamics via synchrosqueezing: prediction of ventilator weaning," *IEEE Transactions on Biomedical Engineering*, vol. 61, no. 3, pp. 736–744, 2014.

[5] R. Amini, J. Herrmann, and D. W. Kaczka, "Intratidal overdistention and derecruitment in the injured lung: a simulation study," *IEEE Transactions on Biomedical Engineering*, vol. 64, no. 3, pp. 681–689, 2017.

[6] K. Roubłk, J. Ráfl, M. van Heerde, and D. G. Markhorst, "Design and control of a demand flow system assuring spontaneous breathing of a patient connected to an HFO ventilator," *IEEE Transactions on Biomedical Engineering*, vol. 58, no. 11, pp. 3225–3233, 2011.

[7] L. Yan, M. Dou, Z. Hua, H. Zhang, and J. Yang, "Optimal duty cycle model predictive current control of high-altitude ventilator induction motor with extended minimum stator current operation," *IEEE Transactions on Power Electronics*, vol. 33, no. 8, pp. 7240–7251, 2018.

[8] Y. Zhang and G. Li, "Non-causal linear optimal control of wave energy converters with enhanced robustness by sliding mode control," *IEEE Transactions on Sustainable Energy*, p. 1, 2019.

[9] Q. Chen, H. Shi, and M. Sun, "Echo state network-based backstepping adaptive iterative learning control for strict-feedback systems: an error-tracking approach," *IEEE Transactions on Cybernetics*, vol. 50, no. 7, pp. 3009–3022, 2020.

[10] S. Wang and J. Na, "Parameter estimation and adaptive control for servo mechanisms with friction compensation," *IEEE Transactions on Industrial Informatics*, vol. 16, no. 11, pp. 6816–6825, 2020.

[11] Y. Zhang, T. Zeng, and G. Li, "Robust excitation force estimation and prediction for wave energy converter M4 based on adaptive sliding-mode observer," *IEEE Transactions on Industrial Informatics*, vol. 16, no. 2, pp. 1163–1171, 2020.

[12] Q. Chen, S. Xie, M. Sun, and X. He, "Adaptive nonsingular fixed-time attitude stabilization of uncertain spacecraft," *IEEE Transactions on Aerospace and Electronic Systems*, vol. 54, no. 6, pp. 2937–2950, 2018.

[13] S. Wang, L. Tao, Q. Chen, J. Na, and X. Ren, "USDE-based sliding mode control for servo mechanisms with unknown system dynamics," *IEEE/ASME Transactions on Mechatronics*, vol. 25, no. 2, pp. 1056–1066, 2020.

[14] X. Gao, X. Ren, C. Zhu, and C. Zhang, "Identification and control for hammerstein systems with hysteresis non-linearity," *IET Control Theory Applications*, vol. 9, no. 13, pp. 1935–1947, 2015.

[15] Y. Zhang, R. Vepa, G. Li, and T. Zeng, "Mars powered descent phase guidance design based on fixed-time stabilization technique," *IEEE Transactions on Aerospace and Electronic Systems*, vol. 55, no. 4, pp. 2001–2011, 2019.

[16] G. Sun, J. Zhao, and Q. Chen, "Observer-based compensation control of servo systems with backlash," *Asian Journal of Control*, 2019.

[17] S. Wang, J. Na, and Y. Xing, "Adaptive optimal parameter estimation and control of servo mechanisms: theory and experiments," *IEEE Transactions on Industrial Electronics*, p. 1, 2020.

[18] G. Xuehui, Z. Wei, W. Shubo, W. Minlin, and R. Xuemei, "A prescribed performance adaptive control for hysteresis Hammerstein system," *Journal of Systems Science & Complexity*, vol. 32, no. 4, pp. 1039–1052, 2019.

[19] Q. Chen, N. Qian, and Y.-R. Nan, "Fixed-time adaptive control for buck converters," *Kongzhi Yu Juece/Control and Decision*, vol. 35, no. 5, pp. 1183–1190, 2020.

[20] J. Na, B. Wang, G. Li, S. Zhan, and W. He, "Nonlinear constrained optimal control of wave energy converters with adaptive dynamic programming," *IEEE Transactions on Industrial Electronics*, vol. 66, no. 10, pp. 7904–7915, 2019.

[21] J. Na, Y. Huang, X. Wu, S.-F. Su, and G. Li, "Adaptive finite-time fuzzy control of nonlinear active suspension systems with input delay," *IEEE Transactions on Cybernetics*, vol. 50, no. 6, pp. 2639–2650, 2020.

[22] S. Wang, H. Yu, J. Yu, J. Na, and X. Ren, "Neural-network-based adaptive funnel control for servo mechanisms with

unknown dead-zone," *IEEE Transactions on Cybernetics*, vol. 50, no. 4, pp. 1383–1394, 2020.

[23] X. Gao, "Adaptive neural control for hysteresis motor driving servo system with Bouc-Wen model," *Complexity*, vol. 2018, Article ID 9765861, 9 pages, 2018.

[24] B. Sun, C. Yang, Y. Wang, W. Gui, I. Craig, and L. Olivier, "A comprehensive hybrid first principles/machine learning modeling framework for complex industrial processes," *Journal of Process Control*, vol. 86, pp. 30–43, 2020.

[25] J. Na, A. S. Chen, Y. Huang et al., "Air-fuel ratio control of spark ignition engines with unknown system dynamics estimator: theory and experiments," *IEEE Transactions on Control Systems Technology*, pp. 1–8, 2019.

[26] A. M. Zou, K. Dev Kumar, and Z. G. Hou, "Quaternion-based adaptive output feedback attitude control of spacecraft using Chebyshev neural networks," *IEEE Transactions on Neural Networks*, vol. 21, no. 9, pp. 1457–1471, 2010.

[27] X. Gao and R. Liu, "Multiscale Chebyshev neural network identification and adaptive control for backlash-like hysteresis system," *Complexity*, vol. 2018, Article ID 1872493, 9 pages, 2018.

[28] G. Sun, X. Ren, and D. Li, "Neural active disturbance rejection output control of multimotor servomechanism," *IEEE Transactions on Control Systems Technology*, vol. 23, no. 2, pp. 746–753, 2015.

[29] M.-F. Leung and J. Wang, "A collaborative neurodynamic approach to multiobjective optimization," *IEEE Transactions on Neural Networks and Learning Systems*, vol. 29, no. 11, pp. 5738–5748, 2018.

[30] R. Levie, F. Monti, X. Bresson, and M. M. Bronstein, "CayleyNets: graph convolutional neural networks with complex rational spectral filters," *IEEE Transactions on Signal Processing*, vol. 67, no. 1, pp. 97–109, 2019.

[31] S. Wang, X. Ren, J. Na, and T. Zeng, "Extended-state-observer-based funnel control for nonlinear servomechanisms with prescribed tracking performance," *IEEE Transactions on Automation Science and Engineering*, vol. 14, no. 1, pp. 98–108, 2017.